REMOTE COMPOSITIONAL ANALYSES OF LUNAR OLIVINES. P. J. Isaacson[1], P. G. Lucey[1], Jessica M. Sunshine[2], Rachel Klima[3], [1]HIGP/SOEST, University of Hawaii, Honolulu HI (isaacson@higp.hawaii.edu), [2]University of MD, [3]JHU/APL (isaacson@higp.hawaii.edu).

Introduction: Olivine is the first mineral to crystallize from typical mafic magmas. It is a useful mineral indicator for the petrogenetic processes that acted on a planetary body, as its composition is indicative of the composition and degree of evolution of both the magma's source region and the magma itself [1]. Olvine is a particularly useful indicator for rocky planetary bodies like the Moon because its composition can be assessed at relatively high spatial resolution using visible to near-infrared (VNIR) spectroscopy analyses. Olivine has been detected across the lunar surface in recent years using VNIR spectroscopy [2-5], but attempts to determine its composition have been limited to restricted, relative, and highly generalized analyses [e.g., 6].

In a previous study, we conducted compositional analyses on selected lunar olivine-rich deposits [6]. However, that study was unable to determine olivine composition (Fo#, defined as (Mg/(Mg+Fe)*100)) quantitatively due to an inability to make direct comparisons with laboratory analyses of olivines with known composition [e.g., 7]. This limitation was largely due to the presence of pronounced space weathering-derived continuum slopes in the remotely-sensed spectra that were absent from the unweathered olivines used to define the trends upon which the compositional assessments are based (see below). In the present study, we present an updated, more quantitative approach for remote analysis of lunar olivine composition.

Data: Our primary dataset is the 85-band VNIR reflectance dataset collected by the Moon Mineralogy Mapper (M^3) on Chandrayaan-1 [8]. This dataset covers the wavelength range of ~500 – 3000 nm, including coverage at 20 nm spectral sampling of the greater 1000 nm where typical mafic minerals (olivine, pyroxene) have diagnostic absorption features [9]. We selected olivine-dominated spectra from several regions using a simple ratio technique (a ratio of the intensity of the 1 and 2 μm absorptions) that highlights the diagnostic olivine absorption feature [e.g., 6]. We also studied a suite of laboratory spectra of synthesized olivine samples [10] that have been synthetically space weathered using Hapke theory [e.g., 11]. The unweathered endmember spectra are shown in Fig. 1. The model spectra were calculated using typical ranges of $npFe^0$ abundance in lunar soils [12-14] so a full suite of model spectra (~10k) were produced from each input spectrum shown in Figure 1. This laboratory suite provides validation for our compositional analysis technique when applied to weathered materials as in the remotely-sensed VNIR data. Compositional information for these samples is provided in Table 1.

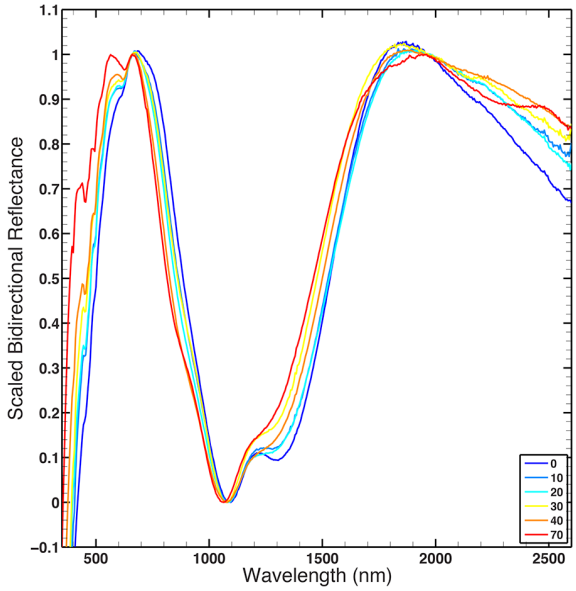

Figure 1: VNIR reflectance spectra of ground truth olivine synthetic olivine samples from [10]. A linear continuum has been removed, and the spectra have been normalized to their maximum band depth near 1000 nm, to facilitate comparisons of spectral properties. Legend indicates nominal composition (Fo#).

Table 1: Compositional data for olivine endmembers

Spl. # / Nom. Comp.	RELAB ID	Meas. Comp.
1 / Fo_0	DD-MDD-098	0.01
2 / Fo_{10}	DD-MDD-097	10.47
3 / Fo_{20}	DD-MDD-096	21.44
4 / Fo_{30}	DD-MDD-095	30.40
5 / Fo_{40}	DD-MDD-042	41.52
6 / Fo_{70}	DD-MDD-039	65.42

Compositional Analysis Technique: Our approach to compositional analysis of olivine-dominated spectra is based on the Modified Gaussian Model (MGM) [15]. It has been applied successfully to laboratory and remote olivine-dominated spectra [7, 16], and also for relative compositional analyses of olivine with M^3 spectra [6]. Our technique is based on the fact that the diagnostic olivine absorption near 1 μm is composed of three component absorptions, which shift in known ways with changing olivine composition (Fo#) [e.g., 17]. The MGM approach is sensitive to initial conditions [18], so we have developed a series of stand-

ard initial conditions (~75) that we apply to each input spectrum. Because of the limited precision and resolution of the M^3 data, precise predictions of composition (i.e., Fo#) are not possible. Our evaluations thus test whether the olivine is Mg-rich (>~Fo_{60}), intermediate (~Fo_{25} - Fo_{75}), or Fe-rich (<~Fo_{40}) by testing initial conditions consistent with each compositional range. The resulting series of fitting solutions is culled for consistency with the known properties of olivine of the composition used as a starting point (i.e., results consistent with Mg-rich olivine for the Mg-rich initial conditions, intermediate for the intermediate initial conditions, etc.), and those results are used to make the compositional assessments (i.e., evaluate the population of valid results consistent with and obtained under each condition). Here, we present results for the synthetically weathered laboratory spectra, which have known compositions, and thus provide an important test for our approach. Further results will be presented.

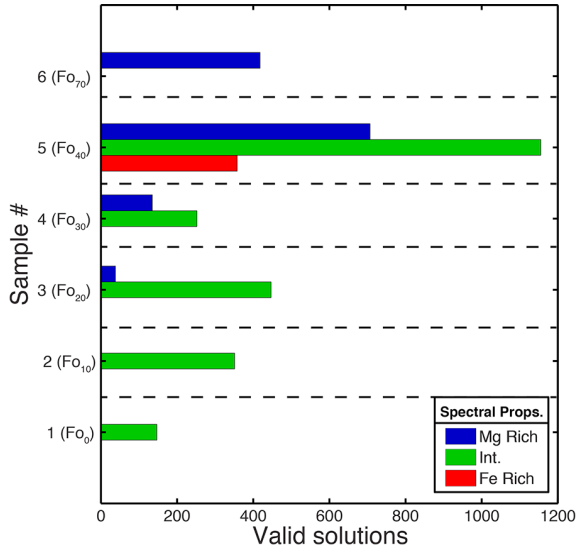

Figure 2: Number of valid fit results under each condition for the weathered lab olivine spectra. Compositions for the samples (which are divided by dashed lines) are as labeled in Fig./Table 1. The proportion of valid results obtained with the Mg-rich initial conditions increases with increasing Fo#. The lack of valid results under the Fe-rich conditions is the subject of further study, as is the Fo_{40} sample.

Results: The results for the laboratory reference spectra are illustrated in Figure 2, which illustrates the count of valid fit results obtained under each of the three initial conditions for each sample. Each endmember spectrum is the seed for a large suite of ~10,000 weathered spectra, so the results indicate that only a relatively small proportion of the input spectra produced valid results. It should be noted that we believe the Fo_{40} sample to be an outlier, and do not discuss those results here. Previous analyses of that spectrum also indicated that it was of lower quality than the others in this suite [10]. Even the Fe-rich samples (Fo_0, Fo_{10}) yield valid results under the intermediate, rather than Fe-rich, conditions. However, as the Fo# of the olivine increases, an increasing number of valid results are produced from the Mg-rich conditions, indicating that the technique is at least generally operating as expected. However, if the technique were operating perfectly, there would be a trend of (proportionally) more Fe-rich results (red in Fig. 1) for Mg-poor samples, trending to more intermediate results (green) for intermediate compositions, and more Mg-rich results (blue) for more Mg-rich samples. This trend is generally observed, particularly for the Mg-rich condition, but the distribution of intermediate and Fe-rich results is less consistent with expectations.

Discussion: While the overall trend observed in Figure 2 is as expected (more valid results obtained from the Mg-rich conditions as the Fo# increases), there are some aspects of the results that require further evaluation or possibly technique modifications. First, none of the spectra yield valid results under the Fe-rich conditions, even for nearly Mg-free olivine samples (Fo_0, Fo_{10}). Even these Fe-rich samples yield valid fits under the intermediate conditions, and we would expect Fe-rich solutions to be more prevalent for those samples. Further work is required to investigate if this is a systematic effect (i.e., that in general, Fe-rich samples might not appear Fe-rich with this technique, perhaps due to our choice of continuum slope in the MGM fits) or if minor adjustments to the initial conditions can improve on this discrepancy. Second, a substantial number of valid results are obtained under multiple compositional conditions (e.g., Fo_{30}). While more results are obtained under the intermediate composition, this is a point that requires further investigation. Third, valid results under the Mg-rich conditions are obtained for samples that would seem to be too Fe-rich for this result (e.g., Fo_{20}-Fo_{30}, whereas Mg-rich results would be expected for samples of >~Fo_{60}). Further investigation is required to determine if this is a systematic effect inherent to our technique (i.e., that a compositional "offset" must be accounted for) or if adjustments can bring this observation more into agreement with expectations.

References: [1] Basaltic Volcanism Study Project (1981). [2] Yamamoto, S. et al. (2010) *Nat. Geosci.*, **3**, 533-536.[3] Yamamoto, S. et al. (2011) *Icarus*, **218**, 331-344. [4] Kramer, G.Y. et al. (2013) *Icarus*, **223**, 131-148. [5] McGovern, P.J. et al. (2013) *LPSC*, **1769**, 6028. [6] Isaacson, P.J. et al. (2011) *JGR*, **116**. [7] Sunshine, J.M. and Pieters, C.M. (1998) *JGR*, **103**, 13675-13688. [8] Pieters, C.M. et al. (2009) *Curr. Sci.*, **96**, 500-505. [9] Burns, R.G. (1993) *Mineralogical applications of crystal field theory*. [10] Isaacson, P.J. et al. (In Press) *AM*. [11] Lucey, P.G. and Riner, M.A. (2011) *Icarus*, **212**, 451-462. [12] Morris, R.V. (1976) *PLPSC*, **7**, 315-335. [13] Morris, R.V. (1978) *PLPSC*, **9**, 2287-2297. [14] Morris, R.V. (1980) *PLPSC*, **11**, 1697-1712. [15] Sunshine, J.M. et al. (1990) *JGR*, **95**, 6955-6966. [16] Sunshine, J.M. et al. (2007) *MAPS*, **42**, 155-170. [17] Burns, R.G. (1974) *AM*, **59**, 625-629. [18] Clénet, H. et al. (2011) *Icarus*, **213**, 404–422.